AIMS Materials Science, 4(5): 1078-1094.
DOI: 10.3934/matersci.2017.5.1078
Received: 27 July 2017
Accepted: 24 September 2017
Published: 11 October 2017

http://www.aimspress.com/journal/Materials

Research article

Ductile fibre reinforced cementitious composites (DFRCC) for improved corrosion durability of reinforced concrete columns

Faiz Uddin Ahmed Shaikh [1,*], Mohamed Maalej [2], and Salah Al Toubat [2]

[1] Department of Civil Engineering, Curtin University, Perth, Western Australia
[2] Department of Civil & Environmental Engineering, University of Sharjah, Sharjah, 27272 UAE

*** Correspondence:** Email: S.Ahmed@curtin.edu.au.

Abstract: This paper reports the results of an experimental program on the effectiveness of ductile fibre reinforced cementitious composites (DFRCC) in retarding the corrosion of steel, corrosion induced damage and post-corrosion structural behaviour of reinforced concrete (RC) columns. Two series RC columns are included in this program. The first series consists of ordinary RC columns that are subjected to an accelerated corrosion regime. The second series consists of two columns that are similar to first two series in every aspect, except that the ordinary concrete in the column is replaced with a ductile DFRCC material. Two types of DFRCC materials are considered: a hybrid-fibre DFRCC containing 1.5 vol.% PVA fibers and 1 vol.% steel fibers and a mono-fibre DFRCC containing 2.5 vol.% PVA fibers. Specimens of the second series are also subjected to a regime of accelerated corrosion. Corrosion damage, including the possible development of spalling and/or delamination, is monitored in each specimen using a specially-fabricated mechanical expansion collar. Based on the collective findings from theoretically-estimated steel losses, visual recordings of corrosion damage, and measurements of the tendency of cover delaminate, it was concluded that the steel reinforced DFRCC columns had a remarkably higher resistance against reinforcement corrosion compared to the ordinary RC columns. The corrosion damaged DFRCC columns also exhibited about 23–64% higher failure load than that of corrosion damaged RC columns and no sign of spalling of cover of columns in the structural test.

Keywords: corrosion; damage; current; reinforced concrete; column; ductile fibre reinforced cementitious composites

1. Introduction

Aging infrastructure facilities, particularly those made of reinforced concrete (RC), are currently deteriorating faster than they are being rehabilitated or replaced. A major cause of concrete deterioration is corrosion of the reinforcing steel in the structure resulting from chloride penetration [1,2,3]. The corrosion of a reinforcing bar in concrete is accompanied by the production of iron oxides and hydroxides, which occupy a volume larger than the original metal. As a result, a large radial pressure is exerted on the surrounding concrete, which may result in local radial cracks. These cracks can propagate along the bar, producing longitudinal cracks, which can result in severe corrosion problems, and leading to general corrosion of the reinforcing bar as the corrosion reaction develops and propagates along the bar. Consequently, a significant bursting pressure is created by the corroded bar resulting in further cracking in the concrete surrounding the rebar and in extreme cases spalling of the concrete, especially at corner bars [4]. When spalling of the concrete cover occurs, the corrosion process accelerates and the reinforced member is likely to experience a loss of strength. Large internal cracks forming along the plane of the corroded reinforcing bars may propagate, resulting in extensive delamination in the structure and seriously compromising its structural integrity [5,6].

Among various techniques to protect or retard the corrosion of steel in concrete, the conventional techniques involve the use of supplementary cementitious materials (SCMs) modified concrete [7,8], the use of fibre reinforced concrete (FRC) [9] and that containing SCMs, the use of low permeable concrete cover, etc. to delay the initiation and propagation of corrosion of steel in concrete. However, the above techniques exhibit limitations in terms of cracking of concrete cover due to shrinkage, thermal stress, and accidental over loads, etc. Even though the FRC or FRC containing SCMs limit the cracking but the width of the cracks increases due their strain softening behaviour during its service life which often exceeds the critical crack width limits for corrosion protection specified in various building codes.

High performance fibre reinforced cementitious composites (HPFRCC) is a kind of cementitious composite materials exhibit strain hardening and multiple cracking behaviour in tension and bending [10]. Engineered cementitious composites (ECC) developed by Li and his co-worker [11], ductile fibre reinforced cementitious composites (DFRCC) proposed by JCI committee [12] and strain hardening cementitious composites (SHCC) proposed by RILEM [13], all belong to the HPFRCC class. One of the most important feature of HPFRCC is its ability to form multiple fine cracks under both tensile and bending loads which are very small in width often below 100 microns [7,14,15,16]. This feature provides the HPFRCC material the ability to prevent the migration of aggressive substances into the concrete even in cracked state. Secondly, in the extreme case when corrosion initiates, the accelerated corrosion due to longitudinal cracks would be reduced (if not eliminated), and spalling and delamination problems common to many of today's RC structures would be prevented. This is expected due to the high ductility and fracture resistance of the HPFRCC material [7,14].

In a number of studies, the effectiveness of HPFRCC in retarding the corrosion of steel and corrosion induced damage in reinforced concrete is evaluated. In the first study, Maalej and Li [17] proposed a new design for RC flexural members where part of the concrete which surrounds the

main flexural reinforcement is replaced with an ECC material. It was found that the widths of flexural cracks were limited to very low below 100 micron which was not achieved using conventional concrete and reinforcing steel. This alternate design with layered ECC had been referred to as Functionally-Grade Concrete (FGC). Subsequently, Maalej et al. [18] evaluated the effectiveness of DFRCC material in retarding the corrosion of steel and corrosion induced damage in medium scale FGC beam. Sahamaran et al. [19] later reported a study where the effectiveness of ECC in corrosion and corrosion induced damage resistance was evaluated in small scale prism specimen. In both studies, the ECC and DFRCC exhibited significantly lower level of corrosion of steel and corrosion induced damage than their control concrete counterpart. Superior corrosion durability of steel in HPFRCC is also reported in several subsequent studies [15,16,20–23]. However, in all above studies small prism specimens were used to study the effectiveness of HPFRCC in retarding corrosion of steel. To translate the success story of HPFRCC from laboratory to real life projects, its implementation in structural member in terms of durability behaviour is important although in Maalej et al.'s study this has been demonstrated in medium scale beams. The corrosion induced damage behaviour of structural member made by HPFRCC and their post-corrosion structural behaviour will be very useful to the designer and asset owners. Motivated by the above results, the author examines in the current study the effectiveness of two types of DFRCCs in retarding the corrosion of steel in reinforced concrete (RC) columns. The two types of DFRCC materials considered include a hybrid-fibre DFRCC (Hy-DFRCC) containing 1.5 vol.% (low modulus) polyvinyl alcohol (PVA) fibers and 1 vol.% (high modulus) steel fibers, and a mono-fibre DFRCC (M-DFRCC) containing 2.5 vol.% PVA fibers. The DFRCCs were introduced as a replacement of the ordinary concrete material of the column for the purpose of retarding the corrosion of steel reinforcement in RC columns and reducing the tendency of the concrete cover to delaminate as measured by a specially-fabricated mechanical expansion collar. The experimental program included 2 RC columns made of ordinary Portland cement concrete and 2 steel reinforced DFRCC columns that are subjected to an electro-chemical accelerated corrosion regime. Post-corrosion structural behaviour and failure of DFRCC columns are also evaluated in this study.

2. Materials and Method

The experimental program consisted of fabricating the four column specimens and allowing them to corrode using an electro-chemical accelerated corrosion technique using constant current while monitoring the progress of corrosion and corrosion damage. The column specimens were intended to simulate possible existing conditions in reinforced concrete bridge columns in which the concrete would be subjected to salt contamination. The test specimens were immersed in (3 percent by weight of water) sodium chloride solution to simulate chloride contamination of the cover by the use of de-icing salt spray. A total of four circular columns were constructed for this study.

2.1. Design of Specimen

The cross sectional details and overall dimensions of a typical column specimen are shown in Figure 1. Incorporated into each column were six 13 mm diameter deformed reinforcing bars,

oriented in the longitudinal direction of the column, and 6 mm diameter spiral at a spacing of 44 mm. A hollow stainless steel pipe with 20 mm diameter and 2 mm thickness was placed longitudinally in the centre of the column to act as a cathode. Holes of 2 mm in diameter were drilled on four sides at 20 mm spacing along the length of the hollow pipe within the test region to increase oxygen exposure. The reinforcing bars were also pre-drilled and tapped at the protruding end to facilitate the electrical connection from the power supply to the specimen. To eliminate any possible end effects, the upper and lower 165 mm sections of the reinforcement cage were coated with epoxy to discourage corrosion.

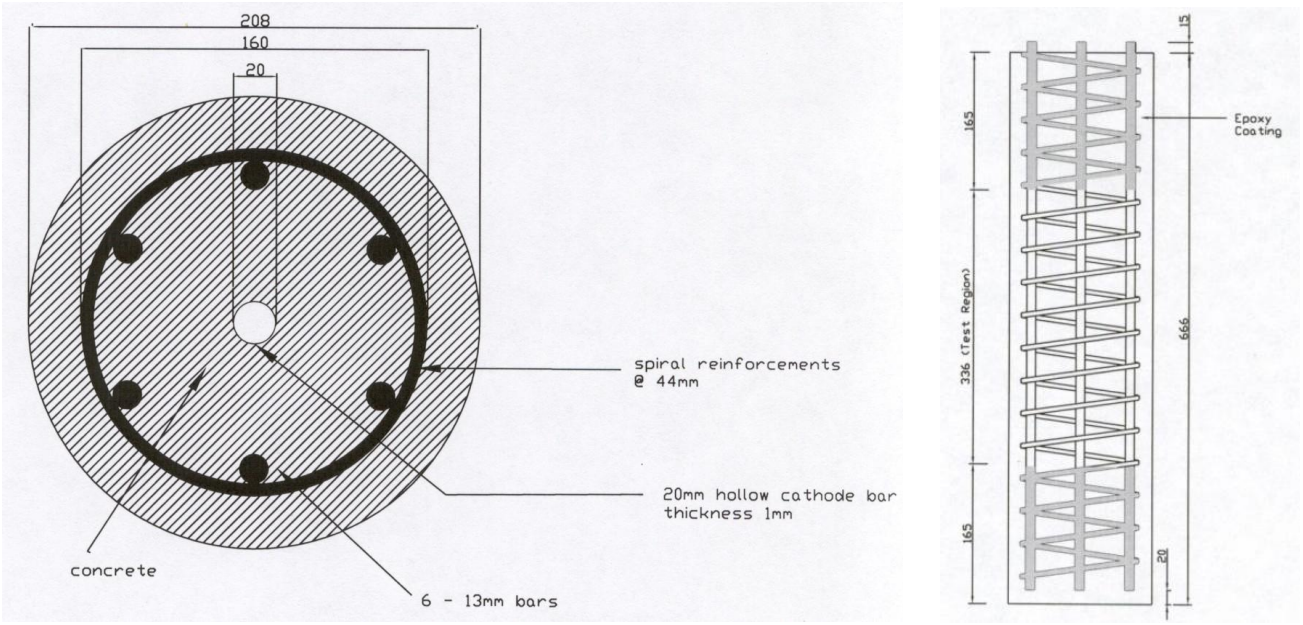

Figure 1. Cross sectional details and overall dimensions of a typical specimen [24].

2.2. Materials

The mix proportions for the OPC concrete and DFRCC are listed in Tables 1 and 2, respectively. Ordinary Portland cement was used for all specimens in this experimental program. Two different types of fibers were used in the casting of the two DFRCC specimens. They were PVA fibers and steel fibers. The properties of these two fibers are summarized in Table 3. The measured average 28-day compressive cylinder strength for the concrete, the hybrid fibre DFRCC and the mono fibre DFRCC were 25.8, 41.8, and 39.9 MPa, respectively. The yield strengths of the 13 mm diameter round deformed bars and 6 mm diameter spiral reinforcing bars were 462 MPa and 285 MPa, respectively. Deflection hardening and multiple cracking behaviour of DFRCC materials in four point bending is also evaluated in 20 × 75 × 300 mm plate specimens for which detail can be found in [25]. Both DFRCCs exhibited deflection hardening behaviour as shown in Figure 2 with higher flexural stress in Hy-DFRCC than that of M-DFRCC due to presence of high modulus steel fibre in the former than the latter.

Table 1. Mix proportions of OPC concrete.

Constituents	Weight (kg/m^3)
Cement (OPC)	300
Water	185
Fine Aggregates	925
Coarse Aggregates (10 mm)	1000
Water	186
Admixture (Duracem-100)	928 ml/m^3

Table 2. Mix proportions of DFRCC.

Constituents (kg/m^3)	Hybrid Steel & PVA Fiber DFRCC (Hy-DFRCC)	Mono Fiber DFRCC (M-DFRCC) (PVA only)
Cement (OPC)	234	234
Water	172	195
Fine Aggregate	460	460
Fly Ash	185	185
Silica Fume	46	46
PVA Fibre	7.38	13.5
Steel Fibre	31.3	-
Super-plasticiser	3846 ml/m^3	3846 ml/m^3

Table 3. Properties of steel and PVA fibers.

Fiber types	Length (mm)	Diameter (μm)	Modulus of Elasticity (GPa)	Strength (MPa)	Density (gm/cc)
Steel	13	160	200	2500	7.8
PVA	12	40	44	1850	1.3

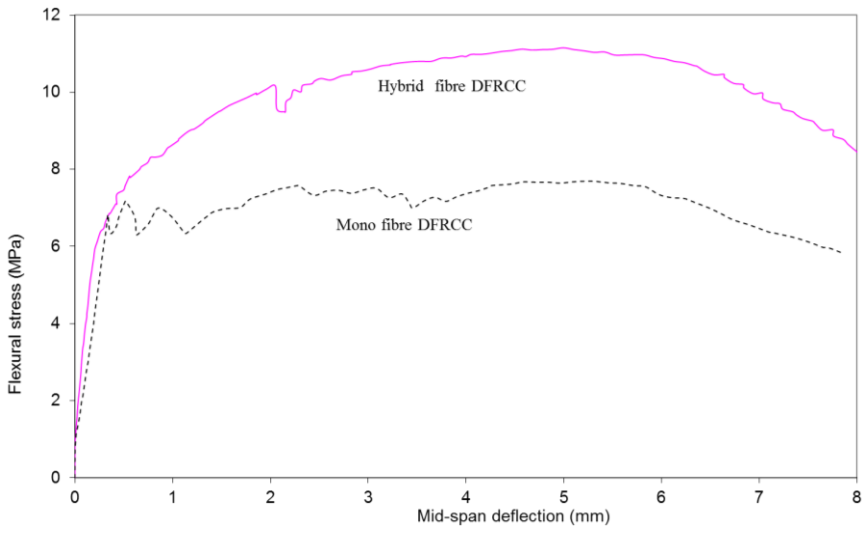

Figure 2. Deflection hardening behaviour of mono and hybrid fibre DFRCC materials.

2.3. Accelerated Corrosion Testing

Four column specimens were subjected to an electro-chemical accelerated corrosion regime using constant current, where the specimens were subjected to cyclic wetting and drying using three percent sodium chloride (NaCl) solution by weight of water while connecting the specimens to a constant current power supply. The cycle was one day wet and two-and-a-half days dry. During the wet cycle, the sodium chloride solution was filled up to the boundary of the upper test region and during the dry cycle, sodium chloride solution was pumped out to below the base level of the specimens. Matsuoka [26] found that a cyclic wetting and drying test is more useful than continuous wetting or immersion in simulating actual field damage within a short time frame.

Figure 3 shows a schematic diagram of the circuit for the accelerated corrosion test. The circuit basically consists of a one-ohm (1 Ω) resistor and the specimen connected in series with the constant current power supply. The 1 Ω resistor and the wires connecting the specimen to the circuit are contained in a specially designed interface box. Wires were also connected from the top of the interface box to a data logger to measure the output voltage readings across the specimen and the 1 Ω resistor. After setting-up and closing the circuits for the accelerated corrosion tests, the voltages across the 1 Ω resistor were recorded on an hourly basis throughout the experiment for a period of about 48 days. According to Ohm's Law (V = IR), the current flowing in the circuit is effectively the same value as the voltage reading since the resistor has a resistance of 1 Ω. By knowing the voltage readings across the specimens, it was also possible to monitor the resistances of all the specimens throughout the experiment since the currents flowing in various circuits were already known.

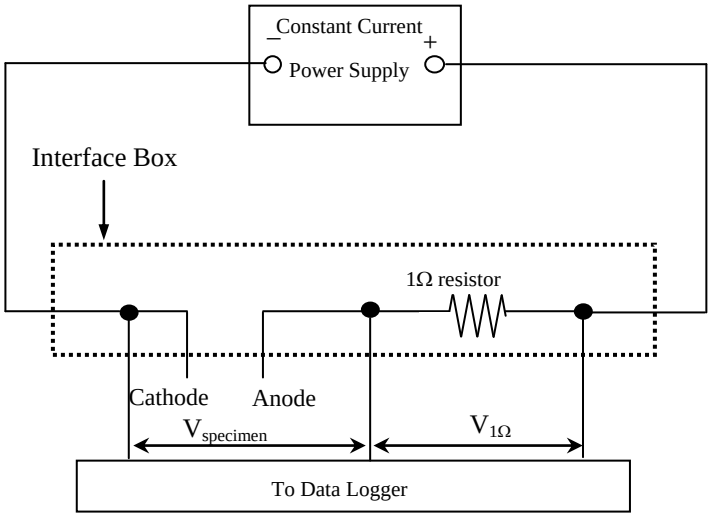

Figure 3. Schematic of the constant current test setup.

The accelerated corrosion process entailed cyclic wetting and drying of the column specimens, which not only provide the necessary moisture for the corrosion reaction, but also a constant fresh supply of chloride ions to the reinforcement bars. Based on a previous study by Lee et al. [27], it was found that a cycle of one day wet and two and a half days dry produces the most corrosion damage to the specimens. Therefore, in the present experiment, the one day (1 D) wet and two and a half days

(2.5 D) dry cycle was adopted. Throughout the experimental program, the corrosion current, circumferential expansion of the specimens and cracking were monitored on a periodic basis. From these, the amount of steel loss Δw calculated based on Faraday's Law using Equation (1), extent of damage caused by the formation of expansive corrosion products and cracking pattern can be determined.

$$\Delta w = \frac{MIt}{zF} \tag{1}$$

Where, Δw = mass of steel consumed due to corrosion (grams);

I = current (amperes);

t = time (seconds);

F = 96,500 (ampere. seconds);

z = ionic charge (2 for Fe);

M = atomic weight of metal (56 g for Fe).

When the specimens are subjected to corrosion, the specimens will expand due to the formation of the corrosion products which are expansive in nature. To measure the circumferential expansion of each column, a specially fabricated mechanical expansion collar (shown in Figure 4) was placed at mid-height of each column. Each collar was made from 12 mm wide stainless steel sheets and included a small opening held closed by two stainless steel springs. A micrometre was used to measure the change in the opening size to the nearest one-hundredth of a millimetre, to determine the circumferential expansion of the column at mid-height.

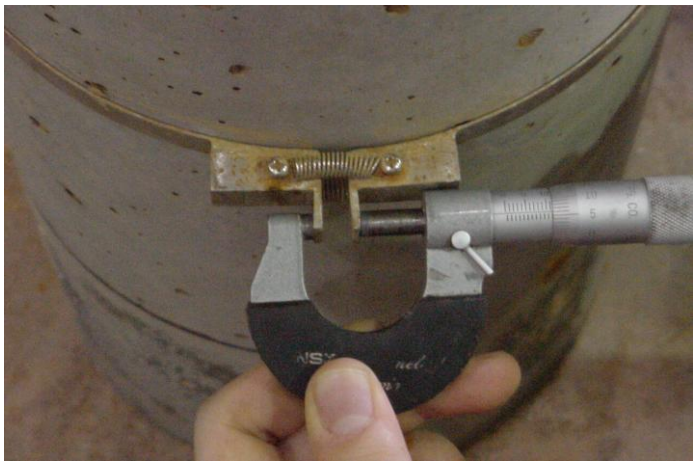

Figure 4. A typical mechanical expansion collar.

3. Results and Discussion

The following sections present the results obtained after about 48 days of accelerated corrosion for the four specimens. Steel loss, circumferential expansion and visual cracking were used as primary indicators of damage. The average percentage steel losses at the end of the accelerated corrosion experiment for RC and the DFRCC specimens were about 8.1% and 2.2%, respectively.

3.1. Applied Corrosion Current

Based on the results of a companion study [27] conducted by the authors on accelerated corrosion of RC columns a magnitude of suppressed current of 0.4 A, giving a current density of 250 μA/cm^2, was initially selected to accelerate the corrosion of all specimens. For the ordinary concrete specimens, this corresponded to an initial applied voltage across the specimen of 9.6 volts. For the DFRCC specimens, a maximum of corrosion current of only 0.1 A could be applied due to a limitation of the constant current power supply unit, corresponding to an applied voltage of 20 volts across the DFRCC specimens. This result gave a preliminary indication that the DFRCC specimens have higher resistance to accelerated corrosion compared to the RC specimens.

3.2. Steel Loss

The accumulated steel loss for the four specimens undergoing accelerated corrosion over time is shown in Figure 5. Steel losses were calculated using Faraday's Law (Eq. (1)). In using Eq. (1), the current efficiency was assumed to be 100% implying that all the current delivered to each specimen is used in the dissociation of iron into ferrous ions, and that the dissociation of iron is only due to the applied current. Heat losses, as well as formation of other independent corrosion cells, are neglected in this experiment. Studies by other researchers have also shown that steel loss calculated using Faraday's Law tends to overestimate the actual steel loss. Aiello [28] determined the actual steel loss gravimetrically and then compared with the calculated steel loss based on Faraday's Law. He found that the calculated values of steel loss were overestimated by 150 to 180%. Recently Paul et al. [29] also reported the overestimation of steel loss by Faraday's law compared to actual steel loss in both ordinary mortar and SHCC specimens. They observed that the difference between the actual steel loss and that estimated by Faraday's law increases with increase in clear cover of concrete and applied voltage.

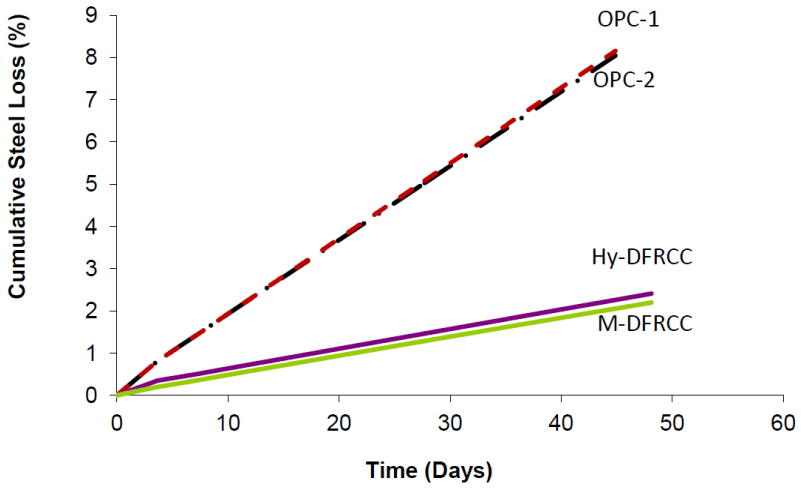

Figure 5. Cumulative steel loss with time.

Despite overestimation of steel loss by Faraday's law, the relative comparison shows significantly lower steel loss in DFRCC columns than that of OPC concrete columns. This is due to lower corrosion current in DFRCC columns than in OPC concrete columns. The more compact microstructure of DFRCC compared to OPC concrete significantly resisted the flow of chloride ions to the reinforcing steel bars during the early stage of corrosion test. With progress of corrosion the formation of cracks on concrete cover due to expansive corrosion products enable easy access of chloride ions in to concrete in OPC concrete columns and accelerated the steel loss which can be seen with significantly higher rate of cumulative steel loss in OPC concrete columns compared to DFRCC columns where due to its deflection hardening and higher fracture resistance characteristics very narrow cracks were formed which significantly lowered the access of chloride ions in to DFRCC and hence, lower rate of cumulative steel loss. By comparing the steel loss between two DFRCC columns it can be seen that the Hy-DFRCC exhibited slightly higher steel loss than its counterpart M-DFRCC. This can be attributed to the lower electrical resistance of Hy-DFRCC due to presence of steel fibres than M-DFRCC as observed in this study which is discussed in next section.

3.3. Circumferential Expansion

Circumferential expansion of each specimen undergoing accelerated corrosion was determined using the specially fabricated mechanical expansion collar fitted at mid height of the column. The circumferential strains at mid height for various specimens over time are shown in Figure 6. From the graph, it can be seen that there was little circumferential expansion for the first 14 days. Subsequently, the OPC concrete columns (OPC-1 and OPC-2) began to show significant increases in the circumferential strain. For the two DFRCC columns, there was little change in the circumferential expansion indicative of minor corrosion activities in these columns. The higher fracture resistance of DFRCC materials than that of OPC concrete also contributed to the lower circumferential strain due to expansive corrosion products developed during accelerated corrosion which is evident from low surface cracking of DFRCC columns observed in this study.

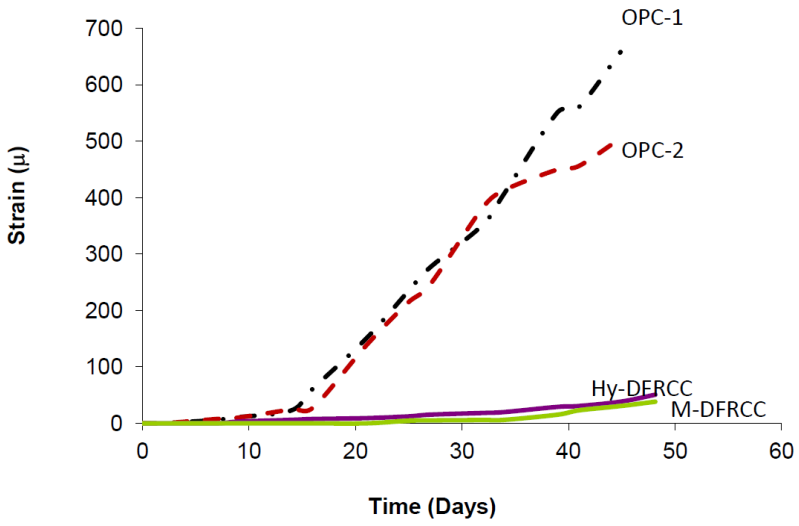

Figure 6. Circumferential expansion with time.

3.4. Electrical Resistances of Specimens

Figure 7 shows the electrical resistances of all specimens with time. It is calculated by dividing the measured voltage with applied current in respective specimens. It can be seen that the electrical resistances of the two DFRCC columns were much higher than those of the OPC concrete columns. This implies that the two DFRCC columns were much more resistant to corrosion than the OPC concrete columns (since corrosion is assumed to be proportional to the current). It was also observed that there were significant increases in the resistances of the two DFRCC columns over time during corrosion test when compared to those of the OPC concrete columns. This may be due to the fact that the cracks that form in the DFRCC columns due to corrosion stay small in width and prevent the corrosion products from escaping to the surface of the specimen. Consequently, the corrosion products slowly build up around the steel bars, preventing more steel from corrosion, which accounted for the increased resistances of the two DFRCC columns. It can also be seen that the electrical resistivity of M-DFRCC column is much higher than that of Hy-DFRCC column. The significantly lower electrical resistivity of Hy-DFRCC column than that of M-DFRCC column can be attributed to the higher electrical conductivity of steel fibre than that of PVA fibre. Similar higher electrical conductivity of steel fibres reinforced concrete is reported by others [30].

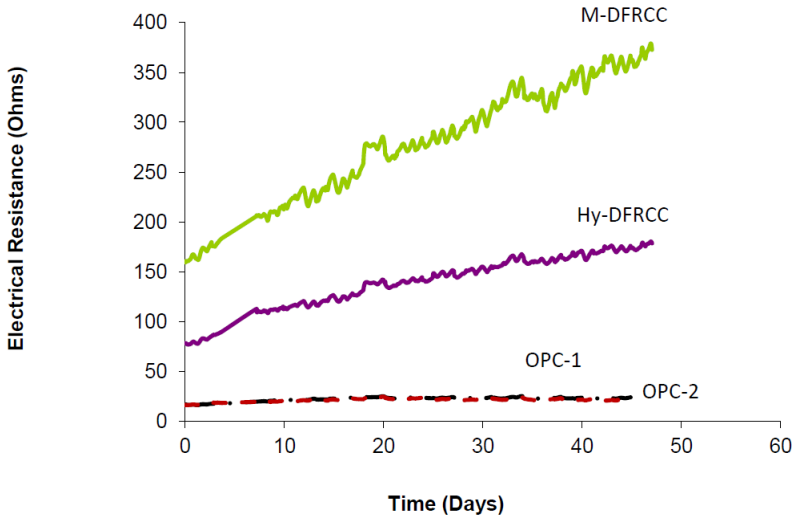

Figure 7. Electrical resistance of specimens with time.

3.5. Surface Staining

Throughout the accelerated corrosion, all four specimens were regularly checked for surface staining and any visual cracks. For the concrete columns, first staining occurred on the surface of the test region and bottom end after about 12 days of accelerated corrosion. The staining was caused by the corrosion products which seeped through small voids and micro-cracks in the concrete during the wet cycle to the surface of the concrete.

For the two DFRCC columns, there was initially no significant surface staining observed. Slight staining of the surface occurred only after about 31 days for both DFRCC columns and the staining

area for both specimens were near the bottom end. The reason could be that the currents for both DFRCC columns were low (0.1 A) when compared to the OPC concrete columns (0.4 A). Therefore, the rate of steel loss in both DFRCC columns was very slow. Consequently, the amount of corrosion products formed was small, hence the tendency for a small amount of corrosion product to seep to the surface is lower than that in the OPC concrete columns. Figure 8 shows the amount of surface staining in the various specimens after 48 days of accelerated corrosion. In the Hy-DFRCC column with steel fibers, it can be seen from Figure 8 that the steel fibers near surface had already rusted.

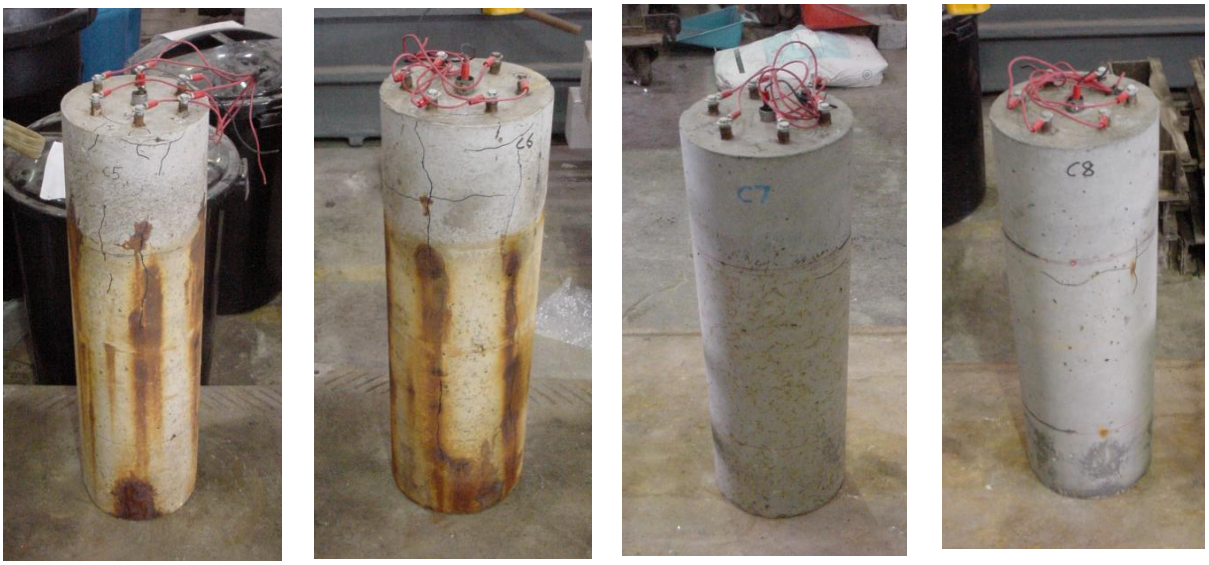

OPC-1 OPC-2 Hy-DFRCC M-DFRCC

Figure 8. Surface staining in RC and DFRCC specimens after 48 days of accelerated corrosion.

3.6. Progression of Cracking Due to Corrosion

As mentioned earlier, the increase in volume of the corrosion products induces internal tensile stress in the concrete cover, and cracking occurs when these stresses exceed the tensile strength of the concrete. The columns were constantly checked for any visual cracks on the surfaces, especially within the test regions. For the OPC concrete columns, visible cracks were observed after approximately 15 days of accelerated corrosion. For these columns, cracks appeared initially as short, vertical and discontinuous near the upper test region. However, as time went by, the cracks began to propagate longitudinally in both directions and some of the vertical cracks joined together. Existing cracks were also seen to be widening. The number and location of each crack was sketched, approximately to scale, on paper as they appeared. Figure 9 shows the crack patterns for all specimens after 48 days of accelerated corrosion.

In addition, horizontal cracks were observed at the upper test region for both columns towards the end of the experiment. Also, there were signs of delamination at the top concrete face where the reinforcement bars protruded for electrical connection for both OPC concrete columns as shown in Figure 9. For both DFRCC columns, the first crack appeared as horizontal crack rather than

longitudinal crack near the upper test region, unlike the OPC concrete columns. The crack began to propagate in the horizontal direction and new horizontal cracks were formed. However, in M-DFRCC column, longitudinal cracks began to appear toward the end of the accelerated corrosion test (see Figure 9).

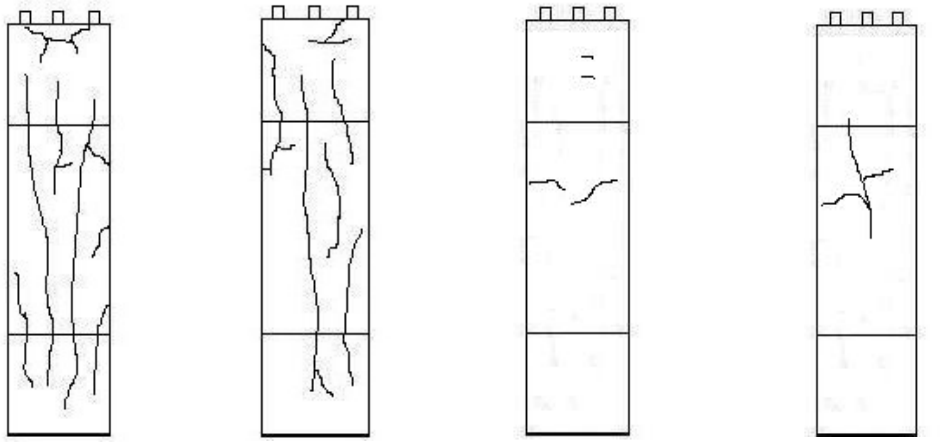

Figure 9. Cracking pattern for RC and DFRCC specimens after 48 days of accelerated corrosion.

Maximum crack width was also measured in all the specimens and a summary of the crack widths measurements at the end of the accelerated corrosion test is given in Table 4. It can be seen that the maximum crack width in OPC concrete columns was 0.46–0.54 mm. On the other hand, in DFRCC columns, it was extremely small 0.08–0.09 mm. For the Hy-DFRCC column the maximum crack width was slightly lower than the M-DFRCC column. This can be attributed to the contribution by high modulus steel fibres in Hy-DFRCC than low modulus PVA fibre in M-DFRCC. Overall the significantly lower crack width in DFRCC columns can be attributed to its deflection hardening and higher fracture resistance than the OPC concrete.

Table 4. Summary of structural test results.

Specimen		Compressive strength (MPa)		Max. Crack Width (mm)
		28 Day	96 Days	
OPC concrete	OPC-1	25.77	28.31	0.54
	OPC-2			0.46
Hybrid Fiber DFRCC	Hy-DFRCC	41.78	46.15	0.08
Mono Fiber DFRCC	M-DFRCC	39.93	45.61	0.09

3.7. Structural Failure Behaviour of Corroded Columns

All corroded columns were structurally tested to evaluate their residual structural load and deformation capacity and compared with un-corroded OPC concrete column. In Figure 10, their residual axial load-axial deformation behaviour is shown. It can be seen that the corroded OPC

concrete columns reduced their axial load carrying capacity by about 4–9%. This can be due to steel loss of longitudinal steel bars due to corrosion, the damage of steel-concrete interface due to corrosion and higher number of longitudinal cracks and spalling of concrete cover due to expansive corrosion products in OPC concrete columns. On the other hand, the corroded DFRCC columns exhibited higher load carrying capacity than un-corroded RC columns. It is found that the corroded Hy-DFRCC and M-DFRCC columns exhibited about 23% and 64% increase, respectively in load carrying capacity than un-corroded OPC concrete columns. The significantly higher residual axial load carrying capacity of both corroded DFRCC columns can be attributed to the higher measured compressive strength than that of OPC concrete. It was found that the compressive strength of DFRCC materials was about 60% higher than its counterpart OPC concrete. As the columns were tested in uni-axial compression, hence, the OPC concrete and DFRCCs contributed mostly to the axial load capacity of their respective columns. It is also interesting to see that all corroded columns exhibited about similar axial deformation capacity at peak load. However, the rate of increase in axial deformation with reduction in axial load was high in DFRCC columns than their counterpart RC columns. This can be due to the presence of coarse aggregates in OPC concrete compared to no coarse aggregates in DFRCC.

Failure behaviour of corroded OPC concrete and DFRCC columns during structural tests is shown in Figures 11–13. It can be seen opening of existing corrosion induced longitudinal cracks in corroded OPC concrete columns in Figure 11 which eventually formed spalling of concrete cover. However, in both DFRCC columns no such spalling of cover concrete is observed, instead multiple cracks are formed during increase in loading and formed few vertical cracks at failure loads which can be seen in Figures 12–13. This might explain the higher failure load of corrosion damaged DFRCC columns than the un-corroded RC column during structural test, which is evident from the spalling of concrete cover as shown in Figure 14. This clearly shows the superior corrosion resistance, corrosion induced damage resistance and structural behaviour of DFRCC columns than that its counterpart OPC concrete column.

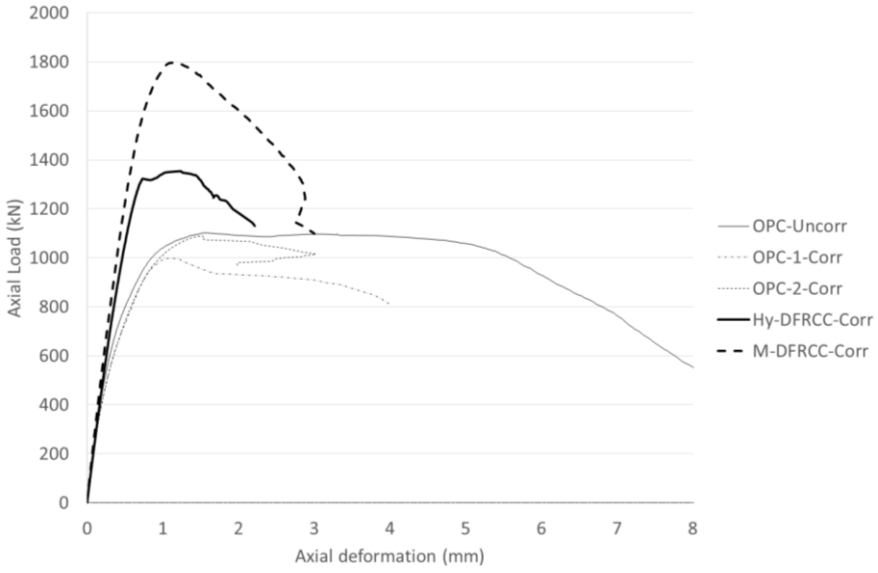

Figure 10. Axial load—deformation behaviour of corroded RC and DFRCC columns.

Figure 11. Spalling of clear cover of OPC-1 and OPC-2 corroded columns after failure load.

Figure 12. Cracking of corroded Hy-DFRCC column during structural test (left) and after failure (right).

Figure 13. Cracking of corroded M-DFRCC column during structural test (left) and after failure (right).

Figure 14. Spalling of un-corroded OPC concrete column at failure during structural test.

4. Conclusions

This paper presented the results of an experimental program on the effectiveness of ductile fibre reinforced cementitious composites (DFRCC) in retarding the corrosion of steel, superior corrosion induced damage resistance and structural response of corroded columns. From the accelerated corrosion regime, it was observed that the OPC concrete columns showed a much lower corrosion resistance and developed significantly higher number of cracks and corrosion stains compared to the DFRCC columns despite the fact that the applied voltages across the DFRCC columns were much greater than those for the OPC concrete columns. Also, the OPC concrete columns showed much greater maximum crack widths and experienced greater circumferential expansion in comparison to the DFRCC columns due to lower tensile/flexural strength and fracture resistance of OPC concrete than its counterpart DFRCC. Considering all these visual indicators of damage, it is clear that OPC concrete columns experienced greater signs of corrosion damage in comparison to the DFRCC columns. Corroded DFRCC columns also exhibited higher (about 23–64%) load carrying capacity than un-corroded OPC concrete column. Corroded DFRCC columns also did not show any sign of spalling at failure. These results show the effectiveness of DFRCC in resisting corrosion and corrosion induced damage in reinforced concrete columns.

Acknowledgments

The support of the Sustainable Construction Materials and Structural Systems (SCMASS) research group, Department of Civil & Environmental Engineering, University of Sharjah is gratefully acknowledged.

Conflict of Interest

There is no conflict of interest.

References

1. Bonacci JF, Maalej M (2000) Externally-bonded FRP for service-life extension of RC infrastructure. *J Infrastruct Syst* 6: 41–51.
2. Guo A, Li H, Ba X, et al. (2015) Experimental investigation on the cyclic performance of reinforced concrete piers with chloride-induced corrosion in marine environment. *Eng Struct* 105: 1–11.
3. Li X, Liang YS, Zhao ZH, et al. (2015) Low-cycle fatigue behavior of corroded and CFRP-wrapped reinforced concrete columns. *Constr Build Mater* 101: 902–917.
4. Gergely P (1981) Role of cover and bar spacing in reinforced concrete. Significant Developments in Engineering Practice and Research, SP-72, American Concrete Institute, Detroit, 72: 133–148.
5. Beeby AW (1978) Corrosion of reinforcing steel in concrete and its relation to cracking. *Struct Eng* 56: 77–81.
6. ACI Committee 224 (1991) Control of Cracking in Concrete Structures, *ACI Manual of Concrete Practice Part 3-1991: Use of Concrete in Buildings-Design, Specifications, and Related Topics*, American Concrete Institute, Detroit.
7. Mehta PK (1999) Advancements in concrete technology. *Concrete Int* 21: 69–75.
8. Ahmed SFU, Maalej M, Paramasivam P, et al. (2006) Assessment of corrosion-induced damage and its effect on the structural behavior of RC beams containing supplementary cementitious materials. *Prog Struct Eng Mater* 8: 69–77.
9. Marcos-Meson V, Michel A, Solgaard A, et al. (2016) Corrosion resistance of steel fibre reinforced concrete—A literature review. Fib symposium—Performance based approaches for concrete structures.
10. Naaman AE (1992) *High performance fibre reinforced cementitious composites*, USA: E & FN Spon.
11. Li VC, Wu HC (1992) Condition for pseudo strain hardening in fibre reinforced brittle matrix composite. *Appl Mech Rev* 45: 390–398.
12. Matsumoto T, Mihashi H (2002) JCI-DFRCC summary report on DFRCC terminologies and application concept. Proceedings of JCI international workshop on ductile fibre reinforced cementitious composites, 59–66.
13. van Zijl GPAG, Slowik V (2017) A framework for durability design of fibre reinforced strain hardening cement based composites (SHCC). RILEM TC240-FDS.
14. Li VC (2003) On Engineered Cementitious Composites. *J Adv Concr Technol* 1: 215–230.
15. Ahmed SFU, Mihashi H (2010) Corrosion durability of strain hardening fibre-reinforced cementitious composites. *Aust J Civil Eng* 8: 27–39.
16. Kobayashi K, Lizuka T, Kurachi H, et al. (2010) Corrosion protection performance of high performance fibre reinforced cement composites as a repair material. *Cement Concrete Comp* 32: 411–420.
17. Maalej M, Li VC (1995) Introduction of strain-hardening engineered cementitious composites in the design of reinforced concrete flexural members for improved durability. *ACI Struct J* 92: 167–176.

18. Maalej M, Ahmed SFU, Paramasivam P (2003) Corrosion durability and structural response of functionally graded concrete beams. *J Adv Concr Technol* 1: 307–316.
19. Sahamaran M, Li VC, Andrade C (2008) Corrosion resistance performance of steel reinforced engineered cementitious composites beams. *ACI Mater J* 105: 243–250.
20. Miyazato S, Hiraishi Y (2005) Transport properties and steel corrosion in ductile fibre reinforced cement composites. Proceedings of the Eleventh International Conference on Fracture, 20–25.
21. Mihashi H, Ahmed SFU, Kobayakawa A (2011) Corrosion of reinforcing steel in fibre reinforced cementitious composites. *J Adv Concr Technol* 9: 159–167.
22. Shaikh FUA, Mihashi H, Kobayakawa A (2015) Corrosion durability of reinforcing steel in cracked high performance fibre reinforced cementitious composite beams. *J Mater Civil Eng* 27.
23. Paul SC, van Zijl GPAG (2014) Crack formation and chloride induced corrosion in reinforced strain hardening cement based composite. *J Adv Concr Technol* 12: 340–351.
24. Altoubat S, Maalej M, Shaikh FUA (2016) Laboratory Simulation of Corrosion Damage in Reinforced Concrete. *Int J Concr Struct M* 10: 383–391.
25. Ahmed SFU, Maalej M, Paramasivam P (2007) Flexural response of hybrid steel-polyethylene fibre reinforced cement composites containing high volume fly ash. *Constr Build Mater* 21: 1088–1097.
26. Matsuoka K (1987) Monitoring of corrosion of reinforcing bar in concrete. Proceedings of the Corrosion '87 Symposium on Corrosion of Metals in Concrete, National Association of Corrosion Engineers, Houston.
27. Lee C, Bonacci JF, Thomas MDA, et al. (2000) Accelerated corrosion and repair of reinforced concrete columns using CFRP sheets. *Can J Civil Eng* 27: 941–948.
28. Aiello J (1996) The effect of mechanical restraint and mix design on the rate of corrosion in concrete [Master's Thesis]. Department of Civil Engineering, University of Toronto.
29. Paul SC, Babafemi AJ, Coradie K, et al. (2017) Applied voltage on corrosion mass loss and cracking behavior of steel reinforced SHCC and mortar specimens. *J Mater Civil Eng* 29.
30. Solgaard AOS, Geiker M, Edvardsen C, et al. (2014) Observations on the electrical resistivity of steel fibre reinforced concrete. *Mater Struct* 47: 335–350.

AIMS Press